

Experimental investigation of the buckling interaction between individual components of a built-up steel stub column

F. Meza, J. Becque

The University of Sheffield

fmezaortiz1@sheffield.ac.uk, j.becque@sheffield.ac.uk

Primary Supervisor: Dr **J. Becque** – e-mail: j.becque@sheffield.ac.uk
Secondary Supervisor: Prof. **J.B. Davison** – e-mail: j.davison@sheffield.ac.uk

ABSTRACT. This paper describes an experimental program carried out at The University of Sheffield on built-up cold-formed steel columns. The columns were constructed from individual channels and plate sections with nominal thicknesses of 1.4 mm and 2.5 mm, respectively. The columns were tested with three different connector spacing and were designed to exclude global instabilities. All the test specimens were compressed between fixed supports and each test was repeated. Therefore, a total of six built-up columns were tested. Coupon tests were extracted from the corners and the flat portions of the sections in order to determine their material properties, and detailed measurements of the out-of-plane imperfections of each specimen were recorded with a laser sensor. These data will be used for the future development of an FE model.

The experiment revealed a pronounced extent of restraint and interaction between the individual components of the section while buckling, with the connector spacing having a significant effect on the observed buckling modes and, to a lesser extent, on the cross-sectional capacity.

KEYWORDS. Built-up column; Experiment; Cold-formed steel; Stability; Buckling; Imperfection measurements.

INTRODUCTION

Cold-formed steel sections have traditionally been used as secondary steelwork in industrial buildings. Common examples are purlins and cladding rails made of lipped channels, sigma or zed sections with thicknesses ranging between 0.5 mm to 6 mm [1]. Depending on the quantity, length and complexity of the sections, they can be produced by roll forming or brake pressing.

The reduced wall thickness of cold-formed steel sections allows for an efficient use of the material, leading to a high strength-to-weight ratio. In addition, due to their shape, they can usually be stacked efficiently, reducing the cost of transportation. They are also easily handled, with single members and sub-frames being easily put in place by operators [1]. All these reasons are leading to an increasing use of cold-formed steel, not just as secondary members, but also as primary load-bearing members, driving the cold-formed steel industry to produce section that can provide larger spans and resist higher loads. Examples of this trend are low-rise multi-storey buildings and cold-formed steel portal frames constructed entirely out of cold-formed steel [2, 3].

On the other hand, the reduced wall thickness of cold-formed steel sections makes them more prone to being affected by cross-sectional instabilities such as local or distortional buckling. These cross-sectional instabilities originate in addition to the global instabilities that are common to the traditionally used hot-rolled sections. Moreover, due to the nature of the fabrication process, the cross sectional shapes that can be cold-formed are commonly mono-symmetric or point-symmetric, with double symmetry difficult to obtain. A logical solution to increase the load carrying capacity of cold-formed steel



members is joining two or more sections together to form a built-up section. Thus, double-symmetric cross sections can be easily constructed with the currently available single shapes. Also, a wider range of cross sectional shapes can be tailored to meet specific requirements.

Despite the benefits built-up sections can offer, the current design codes [4, 5] do not provide any tailored guidance for the design of built-up members. Designing a built-up section requires a careful consideration of various factors, such as the type of connector used, the spacing between the connectors, the degree to which the individual components work as one cross-section, and the occurrence of individual as well as coupled instabilities. A number of experimental tests have previously been carried out on built-up sections. In [6, 7] a series of compressive tests were carried out on closed and open built-up columns made up of two sigma sections connected with screws. The typical I-section made up of two lipped channels connected back-to-back has been extensively studied in [8, 9] where the components were connected using sheet metal screws, and in [10–12] where the channels were welded together. It should be noted that all these tests have only accounted for built-up sections made of two identical components, in which both components buckle at the same time.

The experimental program described in this paper consisted of concentric compression tests on six built-up stub columns. The specimens were assembled by bolting four individual sections together. The program sought to investigate the various instabilities in the members, the interaction between the cross-sectional components during buckling and the effect of the connector spacing on the buckling modes and ultimate capacity of the columns. All columns were tested between fixed supports and were sufficiently short to exclude global instabilities. The specimens were tested with three different connector spacings, and each test was repeated.

SPECIMEN GEOMETRY AND LABELLING

The test specimens were constructed by connecting the flanges of the channels to two plate sections using M6 bolts, as illustrated in Fig. 1. The sections were manufactured from pre-galvanized steel plates with a nominal yield stress of 450 MPa and with a 0.04 mm Z275 zinc coating applied to both sides. All columns had a length of 1100 mm and were designed with 2, 3 or 5 equally spaced connectors. The channels had a nominal thickness of 1.4 mm and the plate sections had a nominal thickness of 2.5 mm. The label used in this paper to refer to each of the built-up specimens consists of the letters ‘SC’ followed by a hyphen and the number of rows of intermediate connectors in the built-up column. As each test was repeated, the letters ‘a’ and ‘b’ indicate whether the specimen was the first or the second of twin columns tested.

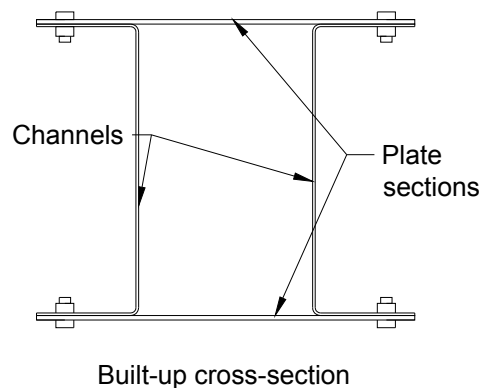


Figure 1: Built-up cross-sectional geometry and individual components

The cross-sectional dimensions of all the individual sections were measured prior to assembling them, and their relative position within the built-up section was recorded. All reported measurements relate to outside dimensions. Tab. 1 lists the measured dimensions and the relative position of the components with reference to Fig. 1, as well as the spacing between connectors of each test specimen.

Both ends of each built-up specimen were manually filed to correct the slight relative difference in length of the individual components. Endplates with dimensions of 250x300 mm² and a thickness of 20 mm were attached at both ends of the column using a 2-part thixotropic epoxy resin. In addition to hand filing the ends, this provided a second means to ensure a uniform introduction of the load into all components.

Column	Channel			Plate		Connector spacing (mm)
	location	Web (mm)	Flange (mm)	location	Width (mm)	
SC-2a	Left	154.00	53.92	Top	199.73	333
	Right	154.23	53.62	Bottom	199.83	
SC-2b	Left	154.13	53.85	Top	199.83	333
	Right	154.13	53.45	Bottom	199.67	
SC-3a	Left	154.23	53.75	Top	199.53	250
	Right	154.10	53.67	Bottom	199.27	
SC-3b	Left	154.17	53.43	Top	199.43	250
	Right	154.10	53.75	Bottom	200.40	
SC-5a	Left	154.17	53.60	Top	200.10	167
	Right	154.17	53.63	Bottom	199.47	
SC-5b	Left	154.13	53.37	Top	198.93	167
	Right	154.23	53.62	Bottom	198.73	
Average		154.15	53.64		199.58	-
St. Dev.		0.07	0.17		0.46	-

Table 1: Measured dimensions of the components and connector spacing

MATERIAL PROPERTIES

Six tensile coupon tests were used to determine the material properties of the individual sections. The coupons were taken in the longitudinal direction, and from spare sections belonging to the same batch as those used in the test. Two identical coupons were taken along the centre line of the plate. In the case of the channels, two identical coupons were extracted from the centre line of the web and other two from the web-flange junction, as the material properties of the channels were expected to differ significantly in the folded region of the cross-section due to plastic deformations induced during the forming process. All coupons were tested following the specification given in the European standard [13]. Tab. 2 lists the average values of the Young's modulus (E), the 0.2% stress ($\sigma_{0.2\%}$) and the tensile strength (σ_u) obtained from each pair of twin coupons.

Type	Section	E (GPa)	$\sigma_{0.2\%}$ (MPa)	σ_u (MPa)
Flat	Plate	195	437	519
Flat	Channel	207	609	704
Corner	Channel	235	609	730

Table 2: Coupon test results.

IMPERFECTION MEASUREMENTS

The stability of thin-walled steel members may be significantly affected by the presence of imperfections. In stub columns, these imperfections are mainly present in the form of out-of-plane deviations of the plates of the sections. Therefore, the imperfections of the most slender plate of each individual component were recorded before testing. Measurements were performed after the built-up columns were assembled into their final configurations, as joining the single sections together might somewhat modify their geometric imperfections.



The equipment used to carry out the measurements consisted of a steel table, a traverse system powered by electric motors and a laser displacement sensor. The arrangement used is shown in Fig. 2. The flat table was guaranteed to be grade 3, providing a flat surface with a deviation from flatness of less than 0.06 mm [14].

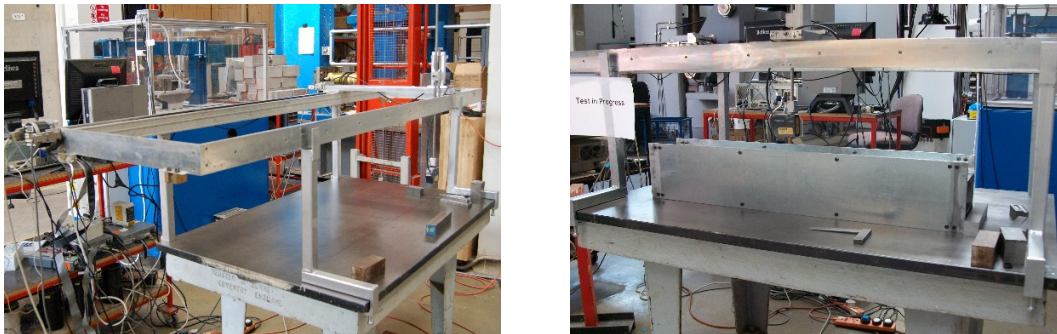


Figure 2: Set-up used to measure the out-of-plane imperfections

To measure the imperfections of the specimens, the traverse system was used to move the laser head along three longitudinal lines on each face of the built-up column at a pre-determined constant speed. Measurements of the imperfections of the plates as well as of the web of the channels were recorded. To correct for the out-of-straightness of the guiding bars along which the laser head was moved, measurements of the table itself were also recorded. Therefore, the accuracy of the measurements was determined by the flatness of the table and can be expected to be of the order of 0.06 mm.

TEST SET-UP

All the specimens were tested between fixed end supports. The specimens were tested in an EHS universal testing machine with a capacity of 1000 kN. The tests were carried out by applying a strain rate of 1.7×10^{-6} /s, resulting in a displacement rate of 0.11 mm/min.

To capture the axial deformations of the specimens and the out-of-plane deformations of their components, 14 LVDTs were employed. Twelve of them were used to measure the out-of-plane deformations of the component sections, and they were placed at mid-distance between connectors. They consisted of two sets of six LVDTs placed at different heights along the column in an attempt to capture the localization of the deformations. The other two LVDTs were placed on each side of the column to measure its axial deformation. The set-up is shown in Fig. 3.

TEST RESULTS

Deformed shape and critical stresses

All test specimens failed due to the interaction of a global-type flexural buckling of the individual plate sections between connectors and local buckling of the channels, as shown in Fig. 3. The presence of the webs of the channels forced the plate sections to buckle mainly outward in all the columns. This may have been accompanied by some slippage in the connectors, as the plates were observed to remain mostly straight in the fields adjacent to the field where the plates buckled outward. The plate sections buckled with a half-wave length larger than half the distance between connectors in all the columns. This implies that the flanges of the channels, at the location of the connectors, had to undergo a certain rotation and translation in order to accommodate the buckling pattern of the plate sections. It is noted that the 'natural' half-wave length of the individual (and unrestrained) channels is 170 mm. By comparing this half-wave length with the actual half-wave length of the channels, observed in the test specimens, it can be concluded that the channels tried to buckle with a half-wave length as close as possible to the 'natural' one, insofar as this buckling configuration was permitted by the buckling pattern of the other components. In the case of columns SC-2 and SC-3, the spacing between connectors was large enough (333 mm and 250 mm respectively) for the channels to accommodate two buckling half-wave between connectors (Fig. 3a and Fig. 3b, respectively). However, in columns SC-5, the spacing between connectors was much shorter and the channels buckled with only one half-wave length between connectors. In these columns, the buckling half-wave length of

the plates coincided with the buckling half-wave length of the channels, which resulted in the flanges of the channels buckling outward in almost perfect sympathy with the plate sections (Fig. 3c).

The critical buckling stresses, of each of the individual sections, obtained from the test were compared with the theoretical values, which were calculated assuming no interaction between the components and using the buckling half-wave lengths observed during the test. In the case of the channels, this buckling half-wave length corresponded to either the distance between connectors or half the distance between connectors. In the case of the plate sections, the buckling half-wave length could not be determined accurately from the experiment and therefore, a lower and upper bound were calculated theoretically, corresponding to assuming that the plate sections buckled with one or two half-waves in between the connectors, respectively. The experimental buckling stresses of the various components were estimated from the LVDT readings. Initially, up to the point of first buckling, the load was transmitted uniformly to all the components. In columns SC-2, the plate sections buckled in a flexural mode before buckling of the channel sections occurred, while simultaneous buckling of the channels and plate sections was observed in columns SC-3 and SC-5. As the plate sections buckled in a flexural mode, it is reasonably assumed that they had no post-buckling capacity and therefore, any further increase of load past the point of buckling was entirely resisted by the channels.

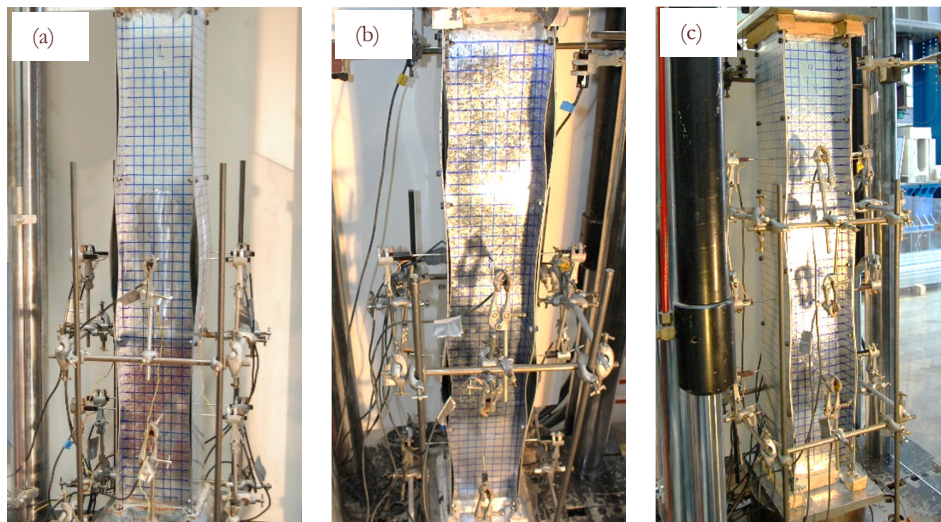


Figure 3: Deformed shape in columns a) SC-2a, b) SC-3a and c) SC-5a.

Column	Theoretical buckling stress (MPa)			Buckling stress from test (MPa)	
	Channel	Plate		Channel	Plate
		Lower	Upper		
SC-2a	63	10	41	52	41
SC-2b	63	10	41	52	41
SC-3a	67	18	73	58	57
SC-3b	67	18	73	56	56
SC-5a	63	41	165	81	81
SC-5b	63	41	165	83	83

Table 3: Theoretical and experimental buckling stresses of the individual sections.

Tab. 3 shows that for columns SC-2 (columns were the plate sections buckled before the channels) the stresses at which the plate sections buckled coincided with the theoretical upper bound, indicating that the channel in its pre-buckled state provided a significant amount of restraint to the plates. The channels, on the other hand, buckled at a stress somewhat lower than the theoretically predicted value. In columns SC-3, simultaneous buckling of the channel and plate sections was experimentally observed. The experimentally derived buckling stress of the channels is slightly lower than the theoretically



predicted value, while the measured buckling stress in the plates is about 23% lower than the theoretical upper bound. In columns SC-5, the channels and the plates sections were also seen to buckle at the same time in the experiment. In this case, the plate sections buckled at a stress well below the theoretical upper bound value, while the channels clearly benefitted from the extra restraint provided by the plate sections and buckled at a stress well above the theoretical value. This is indicative of the fact that the plate and channel sections strongly interacted with each other in these columns and buckled sympathetically with roughly the same half-wave length.

Ultimate load

The ultimate loads obtained for all test specimens, as well as the average values for each set of twin columns, are shown in Tab. 4. Twin columns showed a maximum difference in ultimate load of 8.97% (obtained for columns SC-2). The tests also showed an increase of the ultimate load of the built-up columns as the spacing between connectors was reduced. More specifically, halving the spacing between connectors from 333 mm to 167 mm produced an increase in the ultimate load of 10.81%.

Column	Ultimate load (kN)	Avg. Ultimate load (kN)
SC-2a	183.97	176.07
SC-2b	168.17	
SC-3a	183.01	179.44
SC-3b	175.86	
SC-5a	201.72	195.11
SC-5b	188.50	

Table 4: Ultimate load for test specimens

CONCLUSIONS

Compression tests on six built-up cold-formed stub columns between fixed supports were performed. The investigation included determining the material properties of the specimens through coupons tests, and measuring the specimen out-of-plane imperfections.

The experimental program showed that the different components in the built-up column mutually restrain each other while buckling. This restraint was reflected in the deformed shape which each individual component displayed and in the difference between their theoretical unrestrained and experimentally observed buckling stresses. The restraint was observed to be highly dependent on the connector spacing. However, the impact of the connector spacing on the ultimate capacity of the cross-section was observed to be of lesser importance in these particular cross-sections.

REFERENCES

- [1] Dubina, D., Ungureanu, V., Landolfo, R., Design of Cold-Formed Steel Structures – Eurocode 3: Design of Steel Structures Part 1-3; Design of Cold-Formed Steel Structures, ECCS – European Convention for Constructional Steelwork, first ed, Timisoara Romania, (2012).
- [2] Li, Y., Shen, Z., Yao, X., Ma, R., Liu, F., Experimental investigation and design method research on low-rise cold-formed thin-walled steel framing buildings, *J. Struct. Eng.*, 139 (2013) 818-836.
- [3] Dundu, M., Design approach of cold-formed steel portal frames, *Int. J. Steel Structures*, 11 (2011) 259-273.
- [4] BS EN 1993-1-3, Eurocode 3 – Design of steel structures – Part 1-3: General rules – Supplementary rules for cold-formed members and sheeting, British Standard Institution, (2006).
- [5] AISI, Commentary on North American Specification for the design of Cold-Formed Steel Structural Members, (2007).
- [6] Young, B., Chen, J., Design of cold-formed steel built-up closed sections with intermediate stiffeners, *J. Struct. Eng.*, 134 (2008) 727-737.
- [7] Zhang, J.H., Young, B., Compression tests of cold-formed steel I-shaped open sections with edge and web stiffeners, *Thin-Walled Structures*, 52 (2012) 1-11.

- [8] Lau, H.H., Ting, T.C.H., An investigation of the compressive strength of cold-formed steel built-up I sections, Proceedings of the Sixth International Conference on Advances in Steel Structures. ICASS'09, (2009) 441-449.
- [9] Stone, T.A., LaBoube, R.A., Behavior of cold-formed steel built-up I-sections, Thin-Walled Structures, 43 (2005) 1805-1817.
- [10] Whittle, J., Ramseyer, C., Buckling capacities of axially loaded, cold-formed, built-up C-channels, Thin-Walled Structures, 47 (2009) 190-201.
- [11] Piyawat, K., Ramseyer, C., Kang, T.H., Development of an axial load capacity equation for doubly symmetric built-up cold-formed sections, J. Struct. Eng. 139 (2013) 1-13.
- [12] Weng, C.C., Pekoz, T., compression tests of cold-formed steel columns, Ninth International Specialty Conference on Cold-Formed Steel Structures, (1988).
- [13] BS EN ISO 6892-1, Metallic materials – Tensile testing Part 1: Method of test at ambient temperature, British Standard Institution, (2009).
- [14] BS 817, Specification for surface plates, British Standard Institution, (2008).